



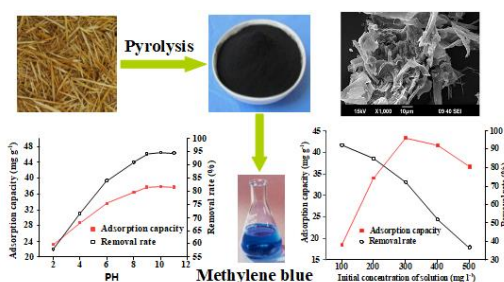
## PREPARATION AND CHARACTERIZATION OF ACTIVATED CARBON DERIVED FROM WHEAT STRAW AND THE ADSORPTION OF METHYLENE BLUE

Guizhen GONG\* and Dandan XIE

School of Materials and Chemical Engineering, Xuzhou University of Technology, Xuzhou 221018, China

Received August 4, 2021

Activated carbon (AC) was prepared from wheat straw through pyrolysis. The AC prepared was characterized by Fourier transform infrared spectroscopy (FTIR), X-ray diffraction (XRD), Brunauer-Emmett-Teller (BET) and Scanning electron microscopy (SEM). The adsorption performance of AC for methylene blue (MB) was examined using a batch method. The effects of different adsorption variables, such as carbonization temperatures, contact time, initial concentration of MB, pH and adsorbent dosage were also evaluated. Carbonization temperatures at 550 °C reach the maximum adsorption value 36.46 mg g<sup>-1</sup>, the adsorption equilibrium time was 115 minutes. The highest adsorption percentage 43.39 mg g<sup>-1</sup> were observed at 300 mg L<sup>-1</sup> concentration of MB, optimum pH value for dye adsorption was determined as 10. With the amount of the adsorbent was increased, the percentage of dye removal increased accordingly. These results show that the AC derived from wheat straw exhibited excellent adsorption performance for MB and can potentially be used for other cationic dyes.



### INTRODUCTION

Activated carbon (AC), with abundant pores, large specific surface area, stable chemical properties, and abundant functional groups,<sup>1</sup> was usually prepared by carbonization and activation processes of carbon raw materials, which has a wide range of uses such as adsorbent, catalysts or catalyst supports, purification, gas storage, etc, and its demand is increasing with the development of industrial and agricultural technology. Traditionally, coal has been used as carbon

precursor to produce AC. However, coal is expensive, limited, and nonrenewable resource. Moreover, the process involves high temperature and high energy consumption, leading to high price of commercial activated carbon. Therefore, it is urgent to find coal substitutes and new technology to fabricate AC. Agricultural waste, as a cheap, renewable, non-toxic, eco-friendly, relatively high carbon content similar to coal, has the potential to produce AC as a substitute for coal

\* Corresponding author: ggz72@163.com

to reduce AC production cost. There are a lot of agricultural wastes in China every year, and are not fully utilized, burned or discarded, which not only wastes resources but also pollutes the environment. Some agricultural wastes, such as rice byproducts,<sup>2</sup> olive residue,<sup>3</sup> fruit stones,<sup>4-7</sup> buriti shells,<sup>8</sup> etc.<sup>9-14</sup> have been successfully prepared into AC by different methods. Basta *et al.*,<sup>15</sup> used rice straw as raw material to prepare activated carbon by carbonization and activation with KOH two-steps method. However, the main disadvantage of alkali activation is the

corresponding low carbon yield. Elmouwahidi *et al.*,<sup>3</sup> prepared AC from a mixture of olive-residue, oil and vegetable water by KOH and H<sub>3</sub>PO<sub>4</sub> activation. H<sub>3</sub>PO<sub>4</sub> activation leads to samples with less surface area than KOH activated carbons but with a more developed mesoporosity. Pezoti Jr *et al.*,<sup>8</sup> reports the preparation of AC produced from buriti shells using ZnCl<sub>2</sub> as activating agent and its ability to remove methylene blue dye (MB) from aqueous solutions. Table 1 presents synthesis of activated carbon from biomass and its applications.

Table 1

Preparation method and application of various AC from biomass			
Raw material	Preparation method	Applications	Refs.
Rice by-products	H <sub>3</sub> PO <sub>4</sub> activation + pyrolysis	MB adsorption	[2]
Shrimp shell	Carbonization, H <sub>3</sub> PO <sub>4</sub> activation	Removal of MB	[16]
Rice Straw and Sewage Sludge	Co-pyrolysis, ZnCl <sub>2</sub> Activation	Removal of Cr(VI)	[17]
Coconut shell	KOH impregnation	Adsorption SO <sub>2</sub> and NO <sub>x</sub>	[18]
Olive stone	ZnCl <sub>2</sub> Activation	Removing Cd(II)	[19]
Rice husk	N <sub>2</sub> -KOH catalyzed pyrolysis	Phenol adsorption	[20]
Palm shell	Carbonization-K <sub>2</sub> CO <sub>3</sub> activation	–	[21]
Bamboo chip	H <sub>3</sub> PO <sub>4</sub> activation	Adsorption CO <sub>2</sub>	[22]
Guava seeds	NaOH Activation	Amoxicillin removal	[6]
Pistachio nutshell	Carbonization, CO <sub>2</sub> or K <sub>2</sub> CO <sub>3</sub> activation	Removal of NO <sub>2</sub> /H <sub>2</sub> S	[7]

Dyes, especially synthetic dyes, are widely used in coatings, plastics, textiles, leather and so on. Synthetic dyes, different from natural dyes, are toxic, stable and difficult to decompose. Approximately 30% of dyes are discharged as effluents into the environment and exist long lifetimes in water bodies to contaminate food chains, bioaccumulation in living organisms, thus resulting in adverse effects on the health of animals and human beings. Therefore, the elimination of dye from effluents requires considerable attention. Numbers of methods, such as photoelectrochemical oxidation,<sup>23-27</sup> biotreatment,<sup>28-30</sup> membrane separation,<sup>31</sup> etc.<sup>32,33</sup> have been applied in dye-containing wastewater treatment. These methods are complex, costly and time-consuming. Adsorption, by contrast, is simple, efficient, fast and cost-effective, and thus is currently the favored approach for treating dye wastewaters.<sup>34-36</sup> Among

the adsorbent materials, AC is one of the most widely used adsorbents. Methylene blue (MB), for example, is a cationic dye with the highest frequency in the dying process of medicine, paper, wood and textiles. In high dose, MB is toxic, and can cause vomiting, shock, paralysis of limbs, muscle tissue necrosis and have mutation. Therefore, it is necessary to treat MB wastewater. Most of commercially available AC are predominantly microporous, and can't be used for MB adsorption. Hussein *et al.*<sup>37</sup> used barley straw as a source to prepare AC and investigated the removal of MB dye from simulated water. They found that the percentage of dye removal increased accordingly as with the increase of adsorption dose, higher adsorption percentages were observed at lower concentrations of MB. Optimum pH value for dye adsorption was as 7 and maximum dye was requested within 90 min after the beginning for every

experiment. Giusto *et al.*<sup>11</sup> produced AC from sugarcane bagasse soot, using CO<sub>2</sub> at 800, 850, and 900 °C, and investigating its efficiency to adsorb MB as model contaminant. The results showed that the activation process resulted in adsorption capacities up to 11 times higher than sugarcane bagasse soot, which is comparable with commercial activated carbon. Macedo *et al.*<sup>38</sup> prepared mesoporous AC from coconut coir dust and investigated the adsorption of MB from aqueous solutions. The results suggested dyes/AC interaction forces are correlated with the pH of the solution, which can be related to the charge distribution on the AC surface.

In the present work, a mesoporous AC was prepared by heating treatment of wheat straw and its application for MB removal was also investigated. Wheat straw (WS) is a common agricultural residue, with a production in China each year about 900 million tons. A small part of wheat straw is used as feedstock, energy source and paper making, of which a large number of incineration, causing serious harm to the environment, traffic. The main components of wheat straw are cellulose, hemi-cellulose and lignin. Due to huge output, high carbon content, low price and renewability, wheat straw is a good option to be used as precursor for producing AC as well as solving the problem of environmental sustainability and reducing the cost of waste management. The preparation of AC adopts one-step pyrolysis below 800 °C and the optimized temperature was 550 °C. Compared with other methods, the temperature is relatively low, which can save energy. The AC prepared was characterized by Fourier transform infrared spectroscopy (FTIR), X-ray diffraction (XRD), Brunauer-Emmett-Teller (BET) surface area method with N<sub>2</sub> adsorption and pore

distribution, and scanning electron microscopy (SEM). The effects of different adsorption parameters, such as carbonization temperatures, contact time, initial dye concentration, pH and adsorbent dosage on the removal of MB on AC were studied.

## RESULTS AND DISCUSSION

### Characterization of the AC

The FTIR spectra of raw wheat straw and AC were employed to detect the changes of vibration frequency in the functional groups. Figure 1 illustrates the FTIR spectra of raw wheat straw and AC-550. In raw wheat straw, the absorption peak at 3237–3600 cm<sup>-1</sup> is due to  $\nu_{(O-H)}$  vibration in hydroxyl group, which split into multiple peaks caused by various intramolecular and intermolecular hydrogen bonds. The peak at 1617 cm<sup>-1</sup> is indicative of aromatic C=C structure bound to unsaturated groups. Absorption at about 1100 cm<sup>-1</sup> was assigned to C-O-C asymmetry stretching. Variations of the FTIR spectra AC-550 was observed in Fig. 1. The band at 3237–3600 cm<sup>-1</sup> which represent the OH stretching vibration became weaker, indicating that cellulose and other components will be coking dehydration and thermal decomposition during high temperature carbonization of wheat straw. In comparison, the absorption band at 1617 cm<sup>-1</sup> and 1100 cm<sup>-1</sup> became stronger, these changes evidence the formation of structures containing multiple carbon-carbon bonds such as aromatic rings, as well as the elimination of originally present oxygen and hydrogen atoms.

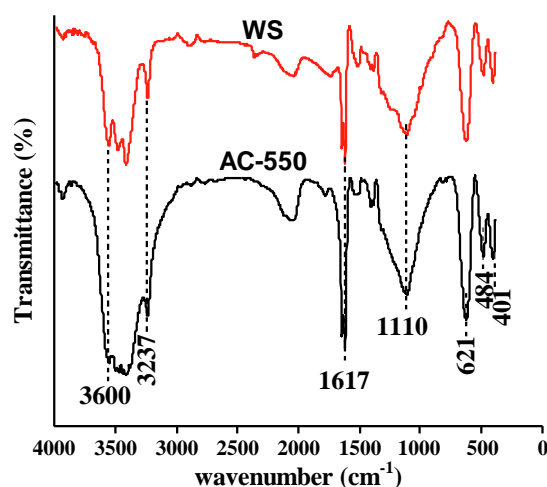


Fig. 1 – FTIR spectra of raw wheat straw and AC-550.

XRD of raw wheat straw and AC-550 are shown in Fig. 2. The diffraction peaks of raw wheat straw are  $2\theta = 15.8^\circ$  and  $22.45^\circ$ . The diffraction peak at  $2\theta = 22.5^\circ$  is strong and sharp, which indicates that the crystal phase integrity of wheat straw is relatively good. In AC-550, the diffraction peaks  $2\theta = 15.8^\circ$  and  $22.45^\circ$  became weaker than that of raw wheat straw, and some new peaks  $2\theta = 27^\circ$  and  $41^\circ$

appear. The diffraction peak  $2\theta = 41^\circ$  is the characteristic of (101) crystal plane of graphite, indicating that AC contains some micro crystalline carbon. The diffraction peak at  $2\theta = 27^\circ$  shows a very wide “Hump” state, and has a tendency to move towards a larger angle, suggesting that the crystal phase of wheat straw is defective after carbonization, and the integrity is severely damaged.

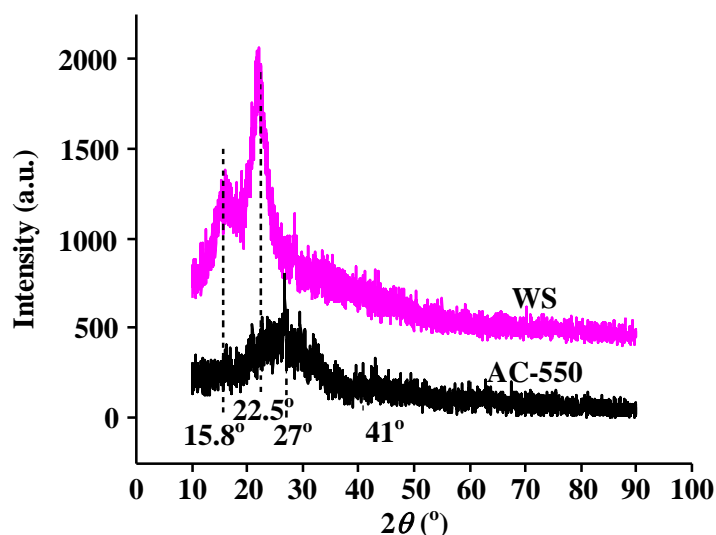


Fig. 2 – XRD of raw wheat straw and AC-550.

Figure 3 shows the nitrogen adsorption-desorption isotherms for AC-550. According to the International Union of Pure and Applied Chemistry (IUPAC) classification, the isotherm is categorized as type IV, together with the presence of a hysteresis loop, which describe mesoporous materials. The total pore volume and  $S_{\text{BET}}$  are  $0.077 \text{ cc g}^{-1}$  and

$17.151 \text{ m}^2 \text{ g}^{-1}$ , respectively. The pore distribution is showed in Fig. 4. The average pore width of  $3.415 \text{ nm}$  is within the mesoporosity range ( $3\text{--}130 \text{ nm}$ ), which are larger than molecule diameter of MB<sup>38</sup>, and thus provide transport channels for its adsorption. So the AC prepared at this process has the potential to purify dye wastewater.

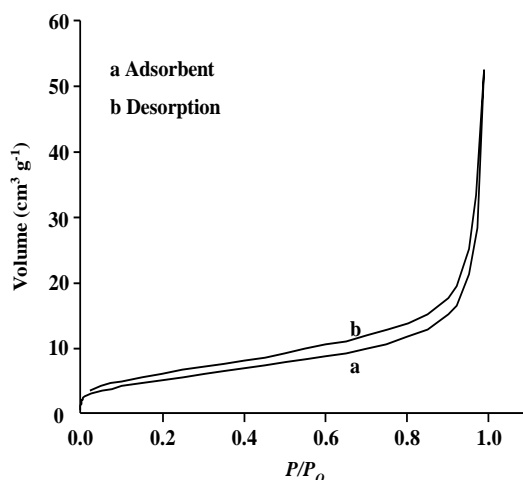


Fig. 3 – N<sub>2</sub> adsorption–desorption isotherm of AC-550 at 77 K.

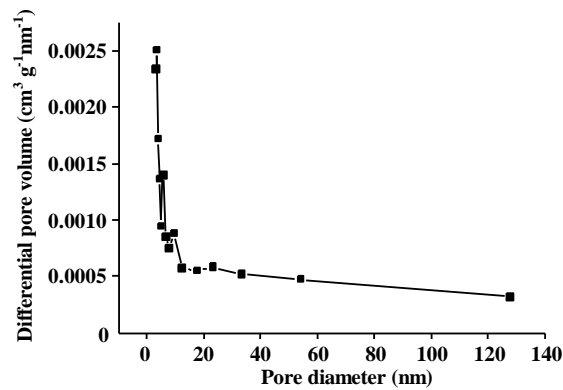


Fig. 4 – BJH method micropore size distribution of AC-550.

The SEM microstructures of raw wheat straw and AC-550 are shown in Fig. 5. Where raw wheat straw (a, b) exhibits a tubular form, regular arrangement with compact, dense, and smooth surface. While AC-550 (c, d) exhibits a loose, soft

and thin, pore structure with the distribution of many irregular cavities on AC surface. This texture is important for adsorption process, because the cavities serve as channels for small molecules.<sup>13</sup>

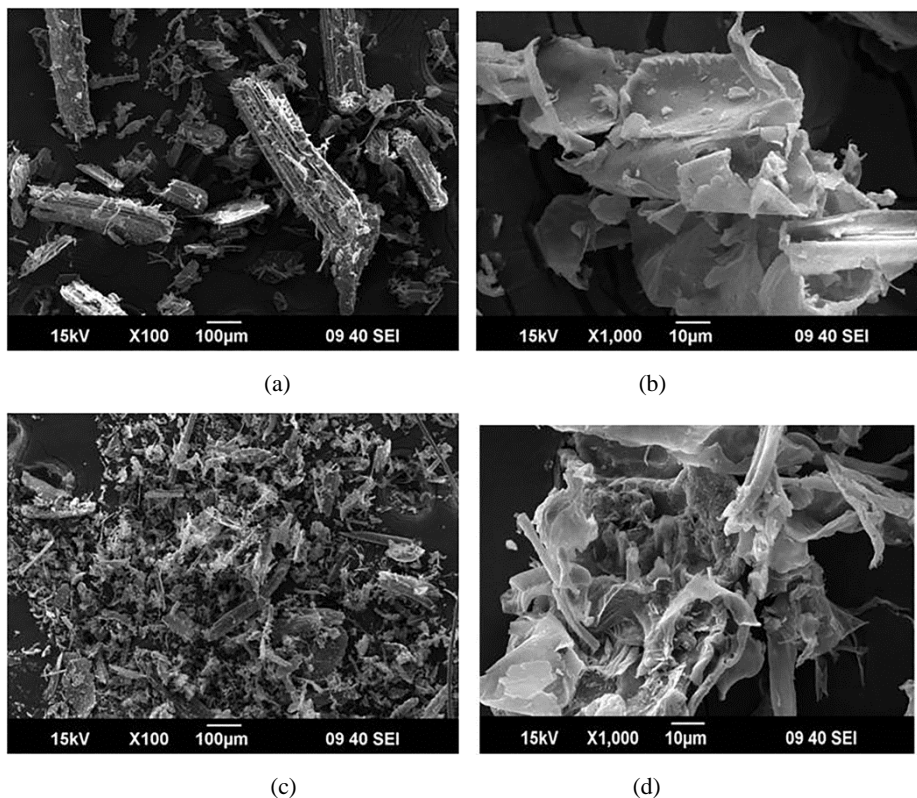


Fig. 5 – SEM images of raw wheat straw (a, b) and AC-550 (c, d).

### Adsorption studies

Effects of carbonization temperature: The effect of carbonization temperatures on the sorption of MB is shown in Fig. 6. A rapid increase in adsorption was initially observed at the temperature range of 300–550 °C, reach the highest 36.46 mg g<sup>-1</sup>

at 550 °C, followed by a gradual decrease with the increase in carbonization temperatures. This may be due to the collapse of the channels formed at too high temperature, resulting in the blockage of the channels and the reduction of the number of pores, which results in low adsorption. So the carbonization temperature of 550 °C is suitable.

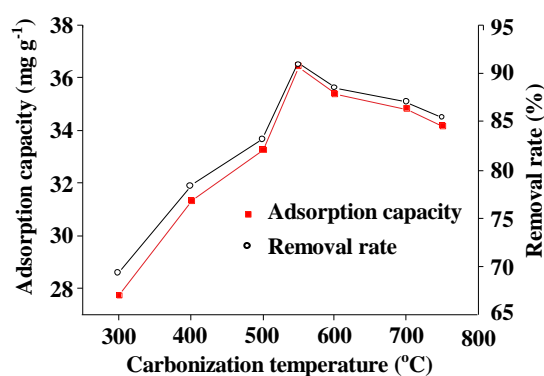


Fig. 6 – Effect of AC prepared at different temperatures on MB adsorption (MB concentration: 200 mg L<sup>-1</sup>; sorbent dose: 0.1 g L<sup>-1</sup>; contact time: 1 h; pH: 10).

Effects of adsorption time: The effect of contact time on the amount of dye adsorbed was investigated, the result obtained is presented in Fig. 7. The adsorption capacity and removal rates exhibit a similar changing process. During the initial stages of the sorption processes, a very rapid

sorption can be observed, then, gradually slow with lapse of time, reached a maximum value at about 115 min and almost become constant with increase in contact time, after 115 min. Hence, it can be said that 115 min is considered the most suitable adsorption time.

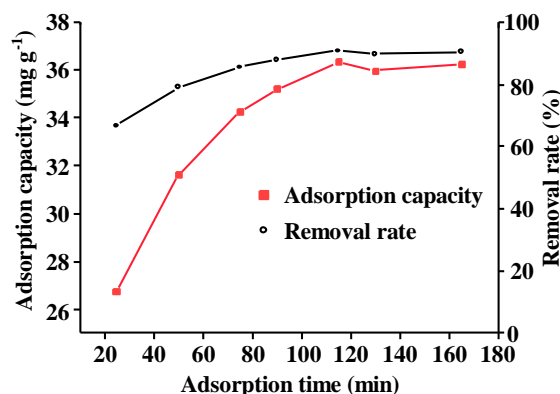


Fig. 7 – Effect of adsorption time on sorption of MB by AC-500 (MB concentration: 200 mg L<sup>-1</sup>; sorbent dose: 0.1 g L<sup>-1</sup>; pH: 10).

Influence of initial dye concentration: The concentration of MB (100, 200, 300, 400, and 500 mg/L) on sorption percentages of MB were presented in Fig. 8. In the range of 100–300 mg / L, the adsorption capacity also increased with the increase of concentration, corresponding to the rapid increase from 18.48 mg g<sup>-1</sup> to 43.39 mg g<sup>-1</sup>. When the dye concentration was increased from 400 to 500 mg g<sup>-1</sup>, the percentage of MB sorbed on AC sharply decreased from 41.63 mg g<sup>-1</sup> to 36.73 mg g<sup>-1</sup>. While, with the increase of MB solution concentration, the removal rate gradually decreased from 92.38% to 36.75%. This may be due to at low concentration, the driving force increases with the increase of concentration, which moves MB towards adsorption sites,<sup>39</sup> but when the

concentration is too high, the molecular size increases to become the main resistance.

Effect of solution pH: Result of pH over range from 2 to 11 on MB dye adsorption is presented in Fig 9. The dye removal ratios were minimal at the initial pH 2. The MB removal ratio of MB increased with the solution pH was increased from pH 2 to 11, the ratio of dye sorbed had neared the maximum value at the solution pH 10. This process may have occurred because the presence of excess H<sup>+</sup> ions holding the sorption sites on AC at low pH, which restrict the approaching cationic MB on adsorbents. When pH increases, a large number of oxygen-containing functional groups on the surface of AC, such as –COOH, are easier to promote dissociation,

which makes the surface of AC show negative charge and form adsorption sites. Consequently, the

adsorption capacity increases. For above reason, the pH 10 was selected for the further experiments.

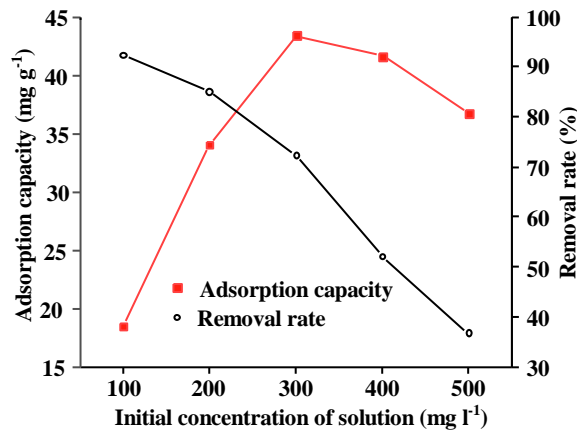


Fig. 8 – Influence of concentration on sorption of MB by AC-550 (sorbent dose: 0.1 g L<sup>-1</sup>; contact time: 1 h; pH: 10).

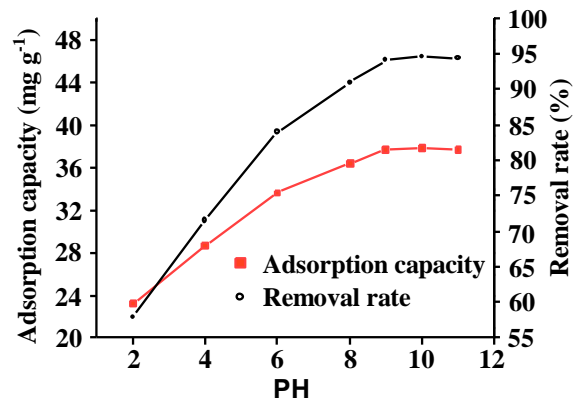


Fig. 9 – Influence of solution pH on sorption of MB by AC-550 (MB concentration: 20 mg L<sup>-1</sup>; sorbent dose: 0.1 g L<sup>-1</sup>; contact time: 1 h).

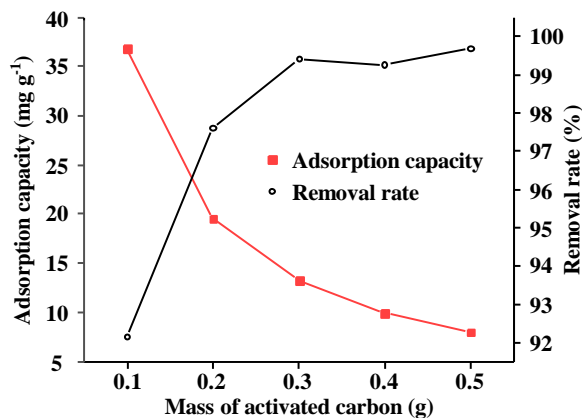


Fig. 10 – Effect of sorbent dose on sorption of MB by AC-550 (MB concentration: 200 mg L<sup>-1</sup> contact time: 1 h; pH: 10).

Effect of sorbent dose: The effects of AC dose on the MB removal ratios were shown in Fig. 10. With the sorbent dose increasing, the MB removal ratios

increased, adsorption capacity of AC decreased. When the AC dose was increased from 0.1 g to 0.3 g, MB removal ratios quickly increased from 92.15%

g to 99.40%, above 0.3 g AC dose, the MB removal ratios only vibrated between 99.25% and 99.69%. This may be attributed to adsorbent surface area and availability of more adsorption sites increased with AC dose increase. However, too much adsorption dose leads to overlapping or aggregation of adsorbent surface area, which makes the methylene blue diffusion path longer.

## EXPERIMENTAL

### Materials

Wheat straw used in this study was collected from the farm at Xuzhou city, Jiangsu, China. The raw material was cut into segment of 3 cm length and rinsed with de-ionized water, and then dried at 100 °C until constant weight. The oven-dried materials were ground, and sieved through 0.25 mm mesh, then stored in a desiccator at room temperature before using.

All chemicals and reagents used were analytical grade and obtained from the commercial source, and were used without further purification.

### Preparation of wheat straw activated

5 g of the raw materials was added in the ceramic disk, and fed into the muffle furnace. The temperature was set in the range of 300–750 °C. After a holding time of 1 h, the furnace was naturally cooled down to room temperature, and the solid residues were collected and rinsed with de-ionized water and ethanol, respectively, then oven-dried at 100 °C for 1 h for further use. The obtained materials were assigned the designation AC-T, where T is the heating temperature (°C) in the muffle furnace.

### Characterization of the activated carbon

FTIR spectra were recorded in the 4000–400  $\text{cm}^{-1}$  region on a ALPH FTIR spectrophotometer (Brooke, Germany) using KBr pellet technique. XRD spectra were performed on Ultima IV (Beijing Science and Technology Co., Ltd, China). The surface morphology of samples were investigated via SEM (SU8010, Hitachi, Japan). Surface area ( $S_{\text{BET}}$ ) and

pore size distribution were calculated with the BET method and Barrett-Joyner-Halenda (BJH) equation, respectively.

### Adsorption tests of methylene blue on AC

The sorption experiments were performed in 250 mL Erlenmeyer flasks at room temperature ( $25 \pm 2$  °C) and containing 50 mL different concentrations and initial pH values of MB solution. MB solution was prepared by dissolving accurately weighted dye in distilled water, the initial concentration of MB in the solution was in the range of 100–500  $\text{mg L}^{-1}$ . The initial pH of the solutions were previously adjusted with dilute HCl or NaOH using a pH meter. Different doses of AC were, respectively, added to each flask, and then the flasks were sealed up and then shaken under magnetic stirring for different time intervals. Then the solutions were separated by centrifugation, the concentrations of MB in the supernatant were determined using ultraviolet spectrophotometer (UV, 722S, Shanghai prism Technology Co., Ltd, China) at 664 nm. The adsorption capacity  $q$  ( $\text{mg g}^{-1}$ ) and removal rate ( $R$ ) were determined by Eqs. (1–2), respectively, as follows:

$$q = \frac{(C_0 - C_1)V}{m} \quad (1)$$

$$R / \% = 100 \frac{C_0 - C_1}{C_0} \quad (2)$$

where  $C_0$  is the initial MB concentration ( $\text{mg} \cdot \text{L}^{-1}$ ),  $C_1$  is the residual MB concentration after adsorption ( $\text{mg L}^{-1}$ ),  $V$  is the volume of the diluent (L) and  $m$  is the mass of AC (g).

## CONCLUSION

Activated carbon were successfully prepared from wheat straw via pyrolysis. The adsorption test of AC for MB removal has been carried out in batch experiment. The adsorption characteristics of AC for MB was dependent on carbonization temperatures, contact time, MB concentration, pH and adsorbent dosage. Higher adsorption value was found for the carbonization temperatures at 550 °C, the adsorption equilibrium was 115 min. The highest adsorption percentage 43.39  $\text{mg g}^{-1}$  were observed at 300  $\text{mg L}^{-1}$  concentration of MB, a pH

of 10.0 is optimal for MB uptake, the MB removal onto AC increased with the amount of the adsorbent. These results show that the AC derived from wheat straw exhibited excellent adsorption performance for MB and can potentially be used for other cationic dyes. These results show that the potential of wheat straw can be used as a source to produce AC as a cost-effective adsorbent to remove cationic dyes from aqueous solution.

*Acknowledgments.* This work was financially supported by China Building Materials Federation (2014-M3-4), Xuzhou University of Technology (XKY2018124).

## REFERENCES

- M. F. R. Pereira, S. F. Soares, J. J. M. órfão and J. L. Figueiredo, *Carbon*, **2003**, *41*, 811–821.
- A. H. Basta, V. F. Lotfy, M. S. Hasanin, P. Trens and H. El-Saied, *J. Clean. Prod.*, **2019**, *207*, 284–295.
- A. Elmouwahidi, E. Bailón-García, A.F. Pérez-Cadenas, F.J. Maldonado-Hódar and F. Carrasco-Marín, *Electrochim. Acta*, **2017**, *229*, 219–228.
- M. J. P. Brito, C. M. Veloso, L. S. Santos, R. C. F. Bonomo and R. da C. I. Fontan, *Powder Technol.*, **2018**, *339*, 334–343.
- P. Nowicki, J. Kazmierczak and R. Pietrzak, *Powder Technol.*, **2015**, *269*, 312–319.
- O. Pezoti, A. L. Cazetta, K. C. Bedin, L. S. Souza, A. C. Martins, T. L. Silva, O. O. Santos, J. V. Visentainer and V.C. Almeida, *Chem. Eng. J.*, **2016**, *288*, 778–788.
- A. Bazan-Wozniak, P. Nowicki and R. Pietrzak, *J. Clean. Prod.*, **2017**, *152*, 211.
- O. P. Jr., A. L. Cazetta, I. P. A. F. Souza, K. C. Bedin, A. C. Martins, T. L. Silva and V. C. Almeida, *J. Ind. Eng. Chem.*, **2014**, *20*, 4401–4407.
- E. D. Ángel-Meraz, H. de J. Orantes-Flores, E. R. Morales and P. Y. Sevilla-Camacho, *J. Mater. Sci. - Mater. Electron.*, **2020**, *31*, 7547–7554.
- F. H. Puspitasari, Nurdiansyah, U. Salamah, N. R. Sari, A. Maddu and A. Solikhin, *Fibers Polym.*, **2020**, *21*, 701–708.
- L. A. R. Giusto, F. L. Pissetti, T. S. Castro and F. Magalhães, *Water Air Soil Pollut.*, **2017**, *228*, 249–259.
- K. Y. Foo, L. K. Lee and B. H. Hameed, *Bioresour. Technol.*, **2013**, *134*, 166–172.
- Y. Ma, Q. Wang, X. Wang, X. Sun and X. Wang, *J. Porous Mater.*, **2015**, *22*, 157–169.
- L. C. A. Oliveira, E. Pereira, I. R. Guimaraes, A. Vallone, A. Pereira, J. P. Mesquita and K. Sapag, *J. Hazard. Mater.*, **2009**, *165*, 87–94.
- A.H. Basta, V. Fierro, H. El-Saied and A. Celzard, *Bioresour. Technol.*, **2009**, *100*, 3941–3947.
- X. Liu, C.Q. He, X.J. Yu, Y. T. Bai, L. Ye, B. S. Wang and L. F. Zhang, *Powder Technol.*, **2018**, *326*, 181–189.
- L.Q. Fan, W. X. Wan, X. D. Wang, J. Cai, F. H. Chen, W. Chen, L. Ji, H. B. Luo and L. Cheng,
- Water Air Soil Pollut.*, **2019**, *230*, 233–246.
- Y. W. Lee, H. J. Kim, J. W. Park, B. U. Choi, and D. K. Choi, *Carbon*, **2003**, *41*, 1881–1888.
- I. Kula, M. Ugurlu, H. Karaoglu and A. Celik, *Bioresour. Technol.*, **2008**, *99*, 492–501.
- Y. Fu, Y. Shen, Z. Zhang, X. Ge, and M. Chen, *Sci. Total Environ.*, **2019**, *646*, 1567–1577.
- D. Adinata, W. M. A. W. Daud and M. K. Aroua, *Bioresour. Technol.*, **2007**, *98*, 145–149.
- Y. Wang, Y. Zhou, C. Liu and L. Zhou, *Colloids Surf., A*, **2008**, *322*, 14–18.
- S. Lan, L. Liu, R. Li, Z. Leng and S. Gan, *Ind. Eng. Chem. Res.*, **2014**, *53*, 3131–3139.
- P. P. Das, A. Roy, M. Tathavadekar and P. S. Devi, *Appl. Catal. B*, **2017**, *203*, 692–703.
- S. Mukhopadhyay, D. Maiti, S. Chatterjee, P. S. Devi and G. Suresh Kumar, *Phys. Chem. Chem. Phys.*, **2016**, *18*, 31622–31633.
- S. Mukhopadhyay, P. P. Das, S. Maity, P. Ghosh and P. S. Devi, *Appl. Catal. B*, **2015**, *165*, 128–138.
- M.R. Sohrabi and M. Ghavami, *J. Hazard. Mater.*, **2008**, *153*, 1235–1239.
- G. Sudarjanto, B. Keller-Lehmann and J. Keller, *J. Hazard. Mater.*, **2006**, *138*, 160–168.
- J. García-Montaño, L. Pérez-Estrada, I. Oller, M. I. Maldonado, F. Torrades and J. Peral, *J. Photochem. Photobiol. A*, **2008**, *195*, 205–214.
- W. Li, B. Mu and Y. Yang, *Bioresour. Technol.*, **2019**, *277*, 157–170.
- J. S. Wu, C. H. Liu, K. H. Chu and S. Y. Suen, *J. Mem. Sci.*, **2008**, *309*, 239–245.
- D. Maiti, S. Mukhopadhyay and P. S. Devi, *ACS Sustain. Chem. Eng.*, **2017**, *5*, 11255–11267.
- L. Fan, Y. Zhou, W. Yang, G. Chen and F. Yang, *Dyes Pigm.*, **2008**, *76*, 440–446.
- S. K. Lakkaboyana, S. Khantong, N. K. Asmel and A. Yuzir, *J. Inorg. Organomet. Polym. Mater.*, **2019**, *29*, 1658–1668.
- F. Marrakchi, M. J. Ahmed, W. A. Khanday, M. Asif and B. H. Hameed, *Int. J. Biol. Macromol.*, **2017**, *98*, 233–239.
- R. M. Gong, Y. B. Jin, J. Sun and K. D. Zhong, *Dyes Pigm.*, **2008**, *76*, 519–524.
- M. Husseien, A. A. Amer, A. El-Maghraby and N. A. Taha, *J. Appl. Sci. Res.*, **2007**, *3*, 1352–1358.
- J. de S. Macedo, N. B. da Costa Júnior, L. E. Almeida, E. F. da S. Vieira, A. R. Cestari, I. de F. Gimenez, N. L. V. Carreño and L. S. Barreto, *J. Colloid Interface Sci.*, **2006**, *298*, 515–522.
- J. M. Salman, V. O. Njoku and B. H. Hameed, *Chem. Eng. J.*, **2011**, *174*, 33–40.

